applied sciences

MDPI

Article

Using Modeling to Select the Type of Microwave Field Emitter for Dense-Layer Grain Dryers

Alexey A. Vasilyev *, Alexey N. Vasilyev and Dmitry Budnikov

Federal Scientific Agroengineering Center VIM, Moscow 109428, Russia; vasilev-viesh@inbox.ru (A.N.V.); dimm13@inbox.ru (D.B.)

* Correspondence: lex.of@mail.ru; Tel.: +7-499-174-85-95

Abstract: The microwave field is used for drying and disinfecting grains during the pre-sowing seed treatment. The use of a microwave field in these installations leads to an increase in their productivity and a decrease in the energy consumed by them. In grain dryers, where the grain moves in a dense layer without being loosened, one of the challenges in using microwave fields is ensuring sufficient uniformity of the field distribution. In this article, waveguide design options that introduce microwave radiation into the grain layer are discussed. The objective of this study was to use application software to find the optimum type of transmitter from the three options presented. A mathematical simulation of the electromagnetic field distribution was performed with the use of CST Microwave Studio software 2019 in order to evaluate and compare horn-type, rectangular, and semicircular waveguides. The data on the standing wave ratio and radiation efficiency of these types of waveguides have been reported. The specific features of the microwave electromagnetic field distribution and radiation power in the output of these waveguides have been described. The results of mathematical simulations revealed that semicircular waveguides with slot-type radiators are preferable for processing dense grain layers.

Keywords: microwave electromagnetic field; waveguide; slot-type radiators; standing wave ratio; radiation efficiency

check for updates

Citation: Vasilyev, A.A.; Vasilyev, A.N.; Budnikov, D. Using Modeling to Select the Type of Microwave Field Emitter for Dense-Layer Grain Dryers. *Appl. Sci.* **2023**, *13*, 9070. https://doi.org/10.3390/app13169070

Academic Editor: José Miguel Molina Martínez

Received: 22 June 2023
Revised: 21 July 2023
Accepted: 2 August 2023
Published: 8 August 2023

Copyright: © 2023 by the authors. Licensee MDPI, Basel, Switzerland. This article is an open access article distributed under the terms and conditions of the Creative Commons Attribution (CC BY) license (https://creativecommons.org/licenses/by/4.0/).

1. Introduction

Normally, wheat grains are subjected to pre-seeding treatment and disinfection with a moisture content of 14%. In order to ensure grain viability and technological quality, grain-drying equipment has to be applied [1]. The initial water content in grains subjected to drying may vary over a wide range, from 18% to 30%. If wet grains are not dried in a timely manner, they will promote the growth of mold and self-heating of the grain. As a result, they become unsuitable for both food and feed purposes. In terms of technological convenience and price, processing plants with thick grain layers are preferable [2], such as hopper-type units [3,4]. Such processing plants are applicable for grain moisture content not exceeding 16%. Processing grains with higher moisture content requires the application of flow-through grain dryers. Depending on the grain crop under processing and the required production rate, various types of grain dryers can be used, such as vertical silage-type dryers [5], tray-type grain dryers [6], free drop flow grain dryers [7], and table-type grain dryers [8].

It should be noted that grain drying is a rather energy-demanding process that accounts for 80% of aggregate energy consumption. That is why various methods designed to reduce the energy consumed for drying, including the application of infrared radiation [9], ozone-air mixtures as drying agents [10], and processing plants with ultrasonic grain drying effect [11] are applied. Grain dryers with alternating blow-through directions in the grain layer [12] and those with grain recycling are also widely used [13]. One of the environmentally safe grain-drying methods is treatment in convective-microwave processing

plants [14,15]. The application of microwaves for processing grains with the purpose of drying, disinfection, and pre-seeding treatment makes it possible to reduce energy consumption and enhance the productivity of the dedicated equipment [16–18]. In the course of pre-seeding treatment, there is a possibility to combine the effect of disinfection with that of improving both the viability of seeds and the yield formula [19,20].

The basic element of such processing plants is the so-called active convective-microwave treatment zone, where waveguides and air ducts are installed. Waveguides serve as microwave radiation conductors, whereas air ducts supply drying agents into the convective-microwave zone [21,22].

One of the principal disadvantages of microwave radiation application for grain processing is defined by the dependence of the penetration depth into the grain layer on the dielectric properties of the materials. The higher the moisture content of the grain, the smaller the distance of its penetration into the grain layer, and the greater the share of microwave power absorbed in the surface sublayer adjacent to the radiation source. At the same time, the maximum productivity of the convective-microwave processing plant can be attained under conditions of uniform interaction between the microwave field and grain.

Previously, the authors designed a shaft-type convective-microwave dryer on the basis of a processing unit in which microwave field sources were installed on the opposite sides of the grain processing zone [23,24] (Figure 1).

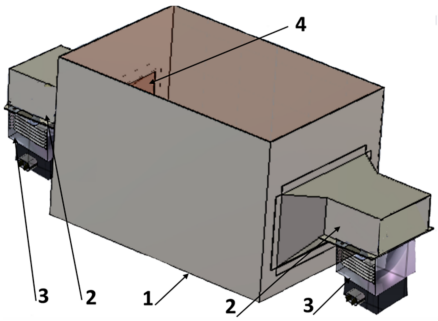

Figure 1. Outlay of convective-microwave zone for grain processing: (1) casing of convective-microwave unit; (2) waveguides; (3) magnetrons; and (4) waveguide output gate.

The unit in the processing plant had the following dimensions 0.3 × 0.2 × 0.2 m, and the volume of the inner space was 0.012 m^3. The length of the active zone, i.e., the distance between the waveguide's output gates, was 0.3 m. The wheat grain weight that could be processed in the convective-microwave zone was 8 kg and 9.1 kg with moisture content of 14% and 25%, respectively.

Small-power magnetrons of 0.9 kW with a radiation frequency of 2.45 GHz are normally used in grain processing units. Radiation is supplied to the microwave-active zone with the help of horn-type antennas. The experimental studies of the grain drying and disinfection processes [25,26] have shown that there is substantial nonuniformity in the electromagnetic microwave field distribution over the grain layer, reducing the efficiency of grain processing. Therefore, there is a need for the development of new design solutions for microwave field introduction into dense grain layers.

The application of rectangular and semicircular waveguides with slot radiators is also regarded as an alternative to horn-type antennas. The use of microwave radiation in grain-processing technology (drying, disinfection, and pre-seeding treatment) has its fundamental peculiarities. These installations cannot be compared to microwave ovens. Each design of microwave grain processing installations typically uses its own radiation-emitting configurations. In the construction of such installations, it is necessary to consider not only the characteristics of the microwave field distribution but also the peculiarities of drying agent delivery to the grain processing zone. For instance, the air can first cool the power blocks and magnetrons before being supplied to the grain layer. In this case, the design of the emitters is of great importance. The choice of emitter configurations can

significantly alter and complicate the construction of the entire installation. This paper considers waveguide configurations that are better suited for convective-microwave grain processing installations with a dense layer. They do not have voids unfilled with grains. The application of the considered waveguide configurations entails specific features and designs of air ducts that deliver hot air to the grain layer in each case. Therefore, the proposed waveguide options are intended for convective-microwave grain-drying installations. Mathematical simulations for the microwave field distribution in the output of such waveguides have been carried out with the use of CST Microwave Studio software [27,28] in order to compare the efficiency of such design types.

2. Materials and Methods

2.1. General Provisions

The analysis of efficiency indicators and the microwave electromagnetic field distribution has been performed for three radiator types, namely: a horn radiator (see Figure 2), a 55 × 110 rectangular waveguide with slot-type emitters (see Figure 3), and a semicircle waveguide with slot-type emitters (Figure 4).

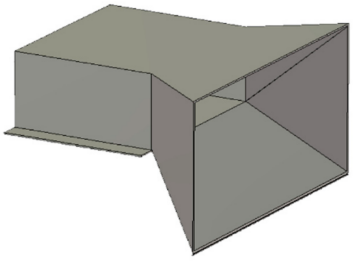

Figure 2. Outlay of the horn-type radiator.

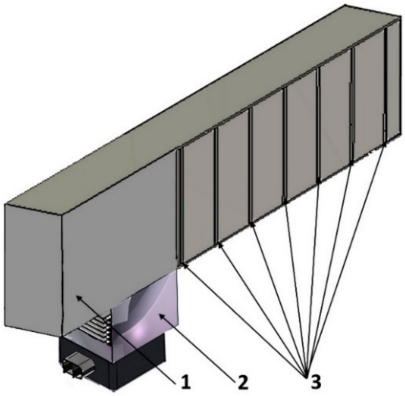

Figure 3. Outlay of 55 × 110 waveguide with slot-type emitters: (1) waveguide casing; (2) magnetron; and (3) slot-type emitters spaced at intervals of $1/2$ λ.

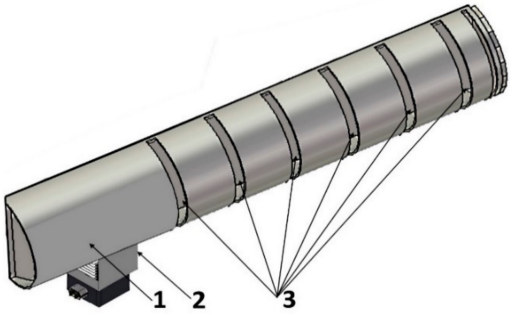

Figure 4. Outlay of semicircle waveguide with slot-type emitters: (1) waveguide casing; (2) magnetron; and (3) slot-type emitters spaced at intervals of $1/2$ λ.

2.2. Methods

The finite method was applied for the mathematical simulation. The finite integration technique (FIT) represents a method of spatial discretization designed for the computational solution of electromagnetic field problems in both time and frequency domains. It makes it possible to retain the basic topological properties of continuous equations such as conservation of charge and energy. The main idea of this approach is to apply the Maxwell equations in their integral form to a multilayer grid.

$$\oint_{(\Gamma)} (H,\, dl) = \int_{(S)} \left(j + \frac{\partial D}{\partial t} \right) dS, \tag{1}$$

$$\oint_{(\Gamma)} (E,\, dl) = -\int_{(S)} \left(\frac{\partial B}{\partial t} \right) dS, \tag{2}$$

$$\oint_{(S)} (D,\, dS) = \int_{V} \rho dV, \tag{3}$$

$$\oint_{(S)} (B,\, dS) = 0, \tag{4}$$

where E is electric field intensity (V/m),
H is magnetic field intensity (A/m),
B is magnetic induction (T),
D is electric induction (Coulomb/m^2),
Γ is borderline enclosing a free-form surface (m^2),
S is free-form surface (m^2),
V is volume (m^3),
j is electric current density (A/m^3),
l is closed contour (m),
ρ is electric charge density (Coulomb/m^3), and
t is time (s).

The major advantages of this method include high flexibility in geometric modeling and boundary processing, and the possibility to involve any material distribution and properties of the material. Additionally, the application of a correlated binary orthogonal grid in combination with an explicit integrating scheme in time yields effective algorithms in terms of the simulation process and storage efficiency.

The essence of the method is based on tiling the computational domain into a finite number of spatial cells. The cells are built so that they completely fit together, and the intersection of two different cells is either a void or a polygon with a one-dimensional edge, or a point shared by both cells (Figure 5).

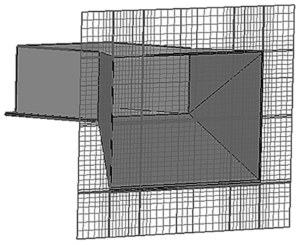

Figure 5. Example of tiling the space in the waveguide output into cells.

Such a partitioning scheme yields the final integration grid that is used as the computation array. Therefore, the entire computation domain is composed of a finite number of elementary cells. Variable electromagnetic fields and flows are normally located along the elementary lines or elementary planes. Similarly, intensities directed along other edges of the cell can be calculated. The aggregate magnetic flow through a plane can be determined as the integral of the magnetic flow density through this plane. As a result, electric field

densities and magnetic flows of the entire cell complex are represented in a matrix form. The solution of this equation yields the desired variables.

In the process of designing microwave devices with the help of CST Microwave Studio 2019 design, structures in a three-dimensional representation are produced by drawing simplest geometric forms (primitives) and by performing logic (Boolean) operations over them [28]. The effectiveness of radiators was evaluated with the use of the following indicators:

- Standing wave ratio (SWR) making it possible to evaluate radiator coherence;
- Radiation efficiency characterizing the share of energy transferred through the waveguide from magnetron;
- Angular pattern of the microwave field. Radiation directionality diagram is drawn in 3D form, which makes it possible to evaluate uniformity of the electromagnetic field distribution in the radiator output;
- The radiation pattern of the microwave field along the waveguide is perpendicular to the radiation;
- Radiated microwave power distribution.

2.3. Features of Electromagnetic Field Transmission by Horn Waveguides

According to the classification, horn antennas belong to the aperture class antennas. They have emitting elements in the form of planar aperture in which angular distribution of the microwave field is achieved. Among advantages of these antennas are a relatively simple and reliable design, convenience of connecting to waveguide transmission lines, rather low energy loss and wide bandwidth [29,30]. Horn antennas are applied in a broad frequency interval ranging from decimeter to millimeter waves. Typical horn antenna design structure is a smooth transition interface between the waveguide's open end and the radiating surface (aperture). The latter is of large size in order to enhance its radiation directionality and, therefore, to attain better matching between the radiator and the feeder transmission line. The authors used a combination of *H*-sectorial and pyramidal horns (see Figure 6a,b). The upper plane of the horn has *H*-sectorial form while the lower one is made in the form of a pyramidal horn (Figure 6c).

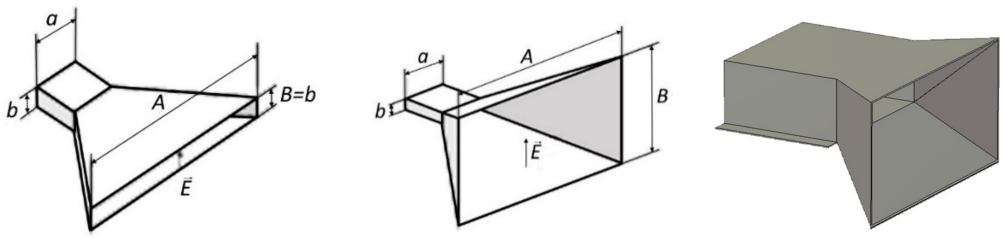

(**a**) (**b**) (**c**)

Figure 6. Horn antennas and the antenna used in the processing plant under studies [13]: (**a**) *H*-sectorial horn; (**b**) pyramidal horn; and (**c**) combined-type horn.

This design is adopted to have the ability to control the direction of the electromagnetic field as it propagates through the grain layer. Since the microwave convective processing system is assembled from modules, one of which is depicted in Figure 1, this waveguide construction allows for directional changes based on the module's position. For instance, when grain enters the upper microwave convective module from the receiving hopper, a downward-directed horn is used. This is done to prevent the microwave field from exiting the system when the grain level in the receiving hopper decreases. In the lower modules of the system, near the discharge hopper, a downward-directed horn is also utilized. This enables the propagation of the electromagnetic field in the lower part of the system.

The opposite direction of the field of the horns in two consecutive zones is used in the lower half of the processing plant, where the moisture content in the processed grain

becomes lower and, consequently, the intensity of the microwave field acting on the grain layer can be increased.

The directional gain (DG) of an aperture-type antenna is defined from the following formula [31]:

$$D = \frac{4\pi S}{\lambda^2}\gamma, \tag{5}$$

where S is the aperture area surface (m^2), λ is the radiation wavelength (m), and γ is the aperture efficiency (AE) depending on the field amplitude and phase distribution in the radiator aperture (a.u.).

The maximum value of AE ($\gamma = 1$) is attained in conditions of uniform and coherent excitation of the aperture.

In a first approximation, the field amplitude distribution in the horn aperture has a sinusoidal form, in the plane of vector H [32]:

$$\frac{E(y)}{E_{max}} \approx \sin\left(\frac{\pi y}{B}\right), \tag{6}$$

where B is aperture area dimension along axis y (m),

$E(y)$ is electromagnetic field intensity along axis y, (V/m), and

E_{max} is the maximum value of electromagnetic field, in the aperture (V/m).

The phase of the field in the aperture changes in accordance with nearly a square law because of the curvilinear form of the wave edge surface. The change in the direction of the electromagnetic field (and its power) at the output of the horn radiator can be described by a second-order equation. The phase displacement has its maximum Φmax on the borders of the aperture area and is equal to:

$$\Phi_{max} \approx \frac{\pi A^2}{4\lambda R}. \tag{7}$$

For a constant length R of the horn, the aperture area S grows with the aperture size A (Figure 7), resulting in decreasing AE due to the increasing phase nonuniformity.

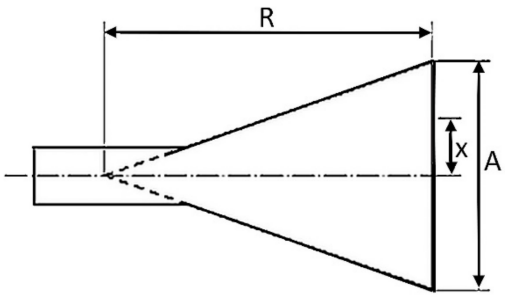

Figure 7. Dimensions used for calculating distortions in the horn aperture [30].

The gain of a horn antenna reaches its maximum at specific values of the aperture size (phase error at the edge of the aperture). For an N-sector horn, this phase error is $3\pi/4$, and such horns are referred to as optimal [33]. The dimensions of optimal horns are determined by substituting the above-mentioned phase shift values into Equation (7) with the above values of phase displacement on the aperture edge: $A = \sqrt{3\lambda R}$, for an N-sector horn. For a frequency of 2.45 GHz, the wavelength is 122 mm. In the horn design, we adopt R = 80 mm, which is the distance from the point of radiation of the magnetron to the end of the horn. Thus, the aperture size $A = \sqrt{3 \cdot 122 \cdot 80}$= 171 mm. However, due to size limitations in the module block construction, where the power supplies and magnetrons are located, A is taken as 88 mm.

In this case, the aperture utilization factor will not be at its maximum. However, it should be noted that the adopted horn aperture design combines H-sectoral and pyramidal

horns. Therefore, a more accurate analysis of the electromagnetic field distribution at the horn exit can be obtained through process modeling.

2.4. Features of Electromagnetic Field Transmission by Rectangular Waveguides

The outlay of the waveguide subject to the electromagnetic field distribution studies is shown in Figure 3. In these studies, a magnetron with an operating frequency of 2.45 GHz was selected as the source of microwave energy. The generator wavelength is equal to [34]:

$$\lambda = \frac{c}{f}, \tag{8}$$

where $c = 3 \cdot 10^8$ m/s is speed of light.

For a frequency value of 2.45 GHz, wavelength is

$$\lambda = \frac{3 \cdot 10^8}{2.45 \cdot 10^9}.$$

$\lambda = 0.122$ m = 122 mm.

In microwave communication devices, the selection of particular wave types such as, H_{10}, H_{01} and E_{11}, is essentially important [35]. Contrariwise, the wave type selection is of no importance when the microwave electromagnetic field is used for heating purposes. It is more critical to ensure loss-free transfer of the radiation to the load. That is why the focus was made on multi-wave guides. Additionally, the dielectric strength of the waveguide can be increased, and the energy loss can be reduced by increasing the dimensions of the waveguide in relation to its length [34]. We will consider wave types capable of transferring along rectangular waveguides. In this regard, let us draw a diagram of critical wavelengths for magnetic and electric-type oscillations.

$$a = 2b, \tag{9}$$

Assuming that a and b are dimensions of the larger and the smaller walls of the rectangular waveguide, respectively.

Critical lengths for the magnetic- and electric-type waves are defined by the following relationship [35]:

$$\lambda_{cr} = \frac{2}{\sqrt{\left(\frac{m}{a}\right)^2 + \left(\frac{n}{b}\right)^2}}, \tag{10}$$

where m and n are oscillation-type indexes H_{mn} (E_{mn}). For E wave, $m \geq 1$, $n \geq 1$. For H-wave, one of the two indexes may be equal to zero [20].

Calculating critical waves for various oscillation types was performed with the use of MATLAB software R2020b [36–38]. In calculations, it was assumed that $a = 1$. When drawing the diagram shown in Figure 8, calculated data were multiplied by the value of a.

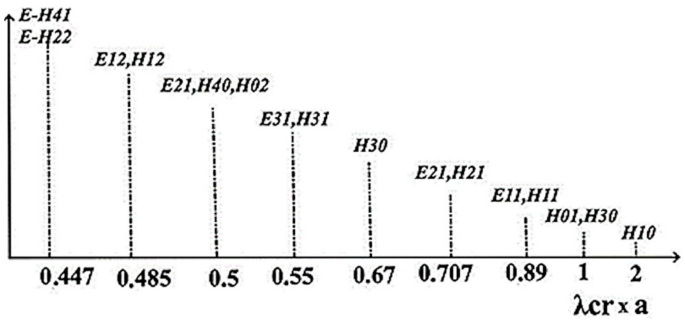

Figure 8. Diagram for oscillation types transferred in the waveguide.

To ensure the possibility of propagation of all modes in waveguides, the following conditions must be observed [39,40]:

$$\lambda < \lambda_{\text{cr}}. \tag{11}$$

For waves of H_{10} type, Equation (7) can be written in the following form:

$$122 < 2 \cdot a.$$

Dimensions of rectangular waveguides stipulated in GOST 51914-2002, for frequencies close to those discussed in this article, are as follows:

Cross-section shall be 110.00 × 55.00 mm and 90.00 × 45.00, respectively, for the frequency ranges from 1.72 GHz to 2.59 GHz and from 2.14 GHz to 3.2 GHz.

Taking into account that, in the processing plant, the microwave field has to be distributed as homogeneously as possible in the grain layer, we assume that the waveguide cross section of 110 × 55 corresponds to this requirement to a greater extent. Therefore, the critical wavelength for this waveguide is $\lambda_{\text{cr}} = 2 \times 110 = 220$ mm. It means that the selected waveguide dimensions comply with Requirement (11).

2.5. Features of Electromagnetic Field Transmission by Semicircular Waveguides

Selection of a semicircle waveguide is, first of all, defined by the specific technological features of the convective-microwave processing. Technical implementation of this method requires the drying agent supply into the area of material processing. With regard to the design convenience, waveguides with a semicircle cross-section are an optimal choice.

The critical wavelength in a circular waveguide, for type E_{mn} wave, can be found from the following equation [27]:

$$\lambda_{\text{cr}} = \frac{2\pi r}{u_{mn}}, \tag{12}$$

or, in application to type H_{mn} wave:

$$\lambda_{\text{cr}} = \frac{2\pi r}{u'_{mn}}, \tag{13}$$

where r is waveguide radius,

u_{mn} are roots of Bessel functions and of their derivatives, for type E wave, and

u'_{mn} are roots of Bessel functions and of their derivatives, for type H wave.

Wave types transferred in circular waveguide, depending on its radius, are presented in Figure 9.

In a waveguide with a semicircle cross-section, as well as in a circular waveguide, the critical wavelength, for type H wave, is λ_{cr} = 3.41 r. For type E wave, λ_{cr} = 1.64 r. It means that, for an inner radius of 50 mm of the waveguide, the critical wavelength, for type H wave, is λ_{cr} = 170 mm, while for type E wave, λ_{cr} = 82 mm. Based on the values of critical wavelengths for a waveguide radius of 50 mm, the propagation of electromagnetic waves of E_{11} type in such waveguides is problematic. Therefore, mainly waves of type H_{11} will go through this waveguide.

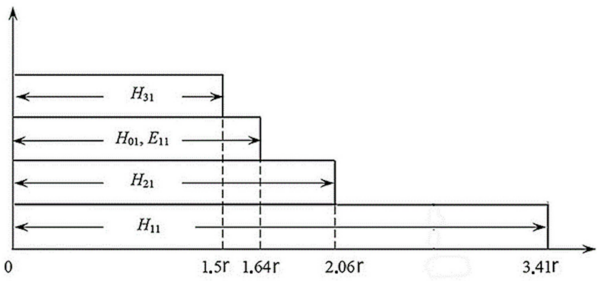

Figure 9. Wave types transferred in circular waveguide.

3. Results

3.1. Studying Microwave Electromagnetic Field Distribution in Horn Antennas

A mathematical simulation of the microwave electromagnetic field distribution process was performed with the use of CST Microwave Studio software. The following parameters were used for the waveguides during the modeling:

For the horn antenna: the cross-section of the rectangular waveguide is 45 × 90 mm; the length of the rectangular waveguide is 104 mm; a short-circuited partition is installed at the end of the rectangular waveguide; the distance from the short-circuited partition to the magnetron output is 1/2 of the wavelength; the length of the horn is 37 mm; and the dimensions of the horn are 148 × 48 mm.

For the rectangular and semi-circular waveguides: the cross-section of the rectangular waveguide is 55 × 110 mm, and the diameter of the semi-circular waveguide is 110 mm; the length of the waveguides with radiating slots is 400 mm; seven radiating slots with a height equal to the length of the lateral surface and a width of 4 mm are located on the lateral side of the waveguides; the distance between the radiating slots is 1/2 of the wavelength; the position of the short-circuited partition to the magnetron output is 1/2 of the wavelength; and the distance from the output of the magnetron to the axis of the first slit is one wavelength.

For all types of radiators, the magnetron output (radiation port) was modeled based on the magnetron's radiating part's dimensions.

The outlay of the horn-type waveguide model used in the mathematical simulation process is shown in Figure 6c.

The frequency ranged from 2 GHz to 3 GHz with central points of 2.45 and 2.5 GHz selected for mathematical simulations. Owing to these selections, a number of dependences were deduced, presented in Figure 10a,b. Figure 10a,b show, respectively, the graph for the frequency dependence of the standing wave ratio (SWR) and that of the radiation efficiency, for the selected horn-type waveguide.

Results of the mathematical simulation show that SWR values fall close to 1.3, for the operating radiation frequency of the magnetron, which is a positive indicator providing evidence of sufficient radiator coherence. Radiation efficiency has a maximum in the radiation frequency range of magnetrons, demonstrating an acceptable level of radiator coherence, as well.

In order to evaluate the electromagnetic field spatial distribution, 3D dependencies were calculated. They are presented in Figure 11.

Results of the 3D mathematical simulations show that there exists a substantial nonuniformity of the electromagnetic field density distribution both along the perimeter of the horn aperture area and in the radiation propagation direction.

Therefore, the application of horn-type waveguides ensures rather high values of SWR (1.3) and high radiation efficiency, but the uniformity of the microwave field density distribution must be improved.

Earlier performed experimental studies [24] have shown that energy consumption of the grain drying process, in convective-microwave zones, essentially depends on the drying agent parameters and on the method of its supply into the grain drying area. Energy consumption can be minimized when the directions of microwave field propagation into the grain layer and that of the drying agent coincide with each other [24]. In this case, a certain grade of microwave field distribution uniformity and that of drying agent concentration, in the grain layer, has to be ensured. This condition is hard to fulfill for the design option of the convective-microwave zone with horn-type waveguides. That is why an attempt was made to develop a waveguide design capable of complying with the above conditions.

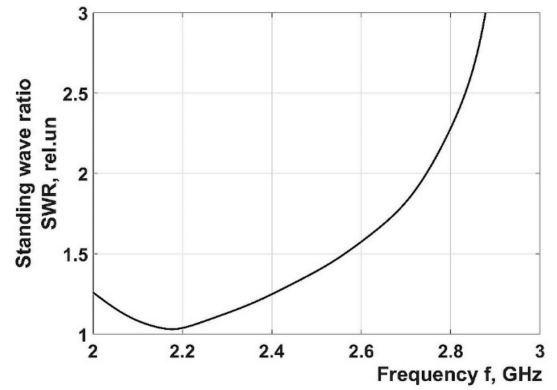

(**a**)

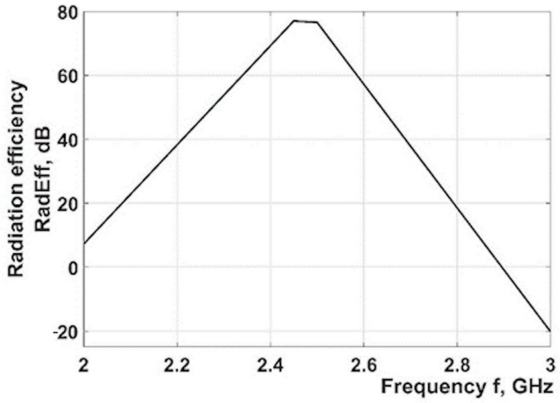

(**b**)

Figure 10. Frequency dependences obtained in the course of mathematical simulations made for microwave field in horn radiator: (**a**) frequency dependence for standing wave ratio (SWR) of the horn-type radiator and (**b**) frequency dependence for radiation efficiency of the horn-type radiator.

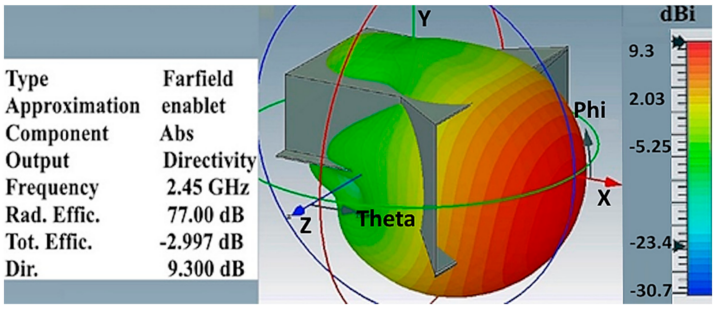

(**a**)

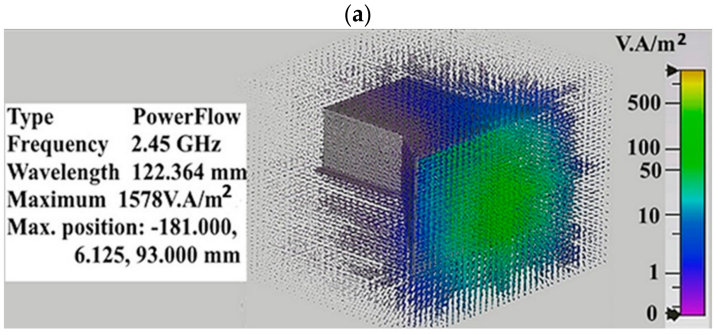

(**b**)

Figure 11. The 3D angular pattern and distribution of radiated microwave power for horn-type waveguide: (**a**) 3D angular pattern for microwave electromagnetic field and (**b**) 3D distribution of the radiated microwave field.

3.2. Studies of Rectangular Waveguides with Slot Radiators

On the basis of this waveguide, a slot radiator was designed [34,41]. For this purpose, transverse slots were cut in the broad waveguide's wall. The transverse slot in the broad wall of the waveguide becomes excited by the direct-axis component of the current. On account of the required volume of the section, a radiator length of 400 mm was selected. Slots in the back side of the radiator are spaced $1/2\ \lambda$ apart (Figure 3).

Radiator parameters were first conformed and then were input into CST Microwave Studio software for mathematical simulation of the electromagnetic field distribution from the radiator's slots. The results of this simulation are presented in Figures 12 and 13.

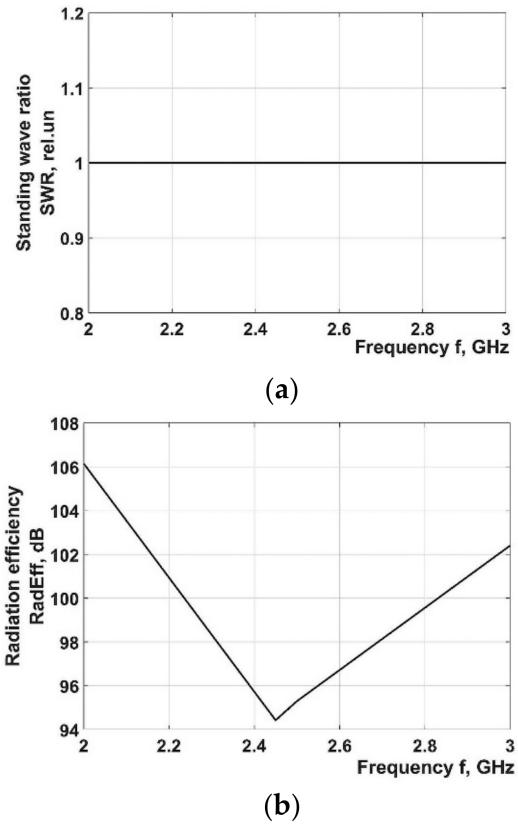

Figure 12. Frequency dependences obtained by mathematical simulation for microwave field in rectangular (55 × 110) radiator: (**a**) frequency dependence of the standing wave ratio (SWR) for rectangular slot type radiator and (**b**) frequency dependence of the radiation efficiency for rectangular slot radiator.

Mathematical simulation results show that the application of a rectangular waveguide makes it possible to achieve better homogeneity of the electromagnetic field distribution. Additionally, the rectangular waveguide features SWR equal to 1 and increased radiated power values.

That is why the use of a rectangular 55 × 110 waveguide in convective-microwave zones for processing grain is more preferable.

Apart from the rectangular 55 × 110 waveguide, mathematical simulation of the electromagnetic field distribution was performed for a waveguide with a semicircle cross-section (circular sector) and a slot radiator (Figure 4).

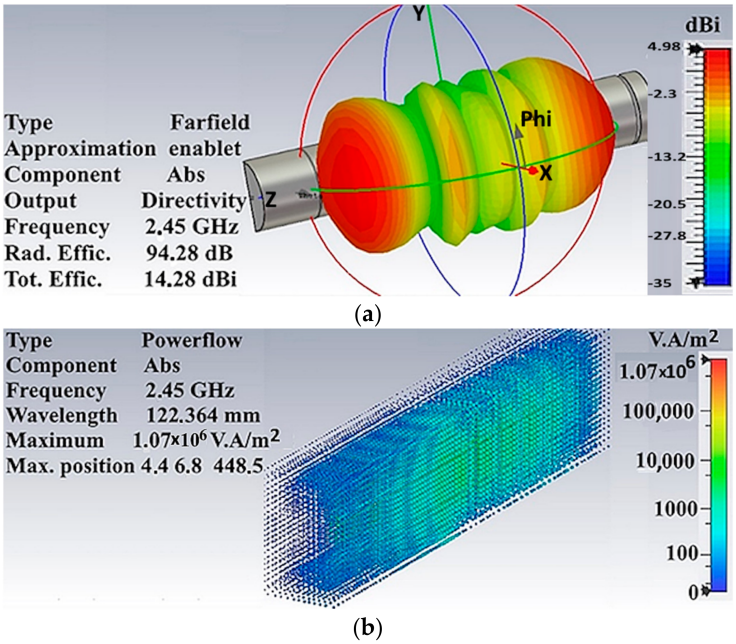

Figure 13. The 3D angular patterns of directionality and distribution of radiated power for rectangular 50 × 110 waveguide: (**a**) 3D angular pattern of microwave electromagnetic field for rectangular slot-type radiator and (**b**) 3D diagram of microwave field density distribution for rectangular slot-type radiator.

3.3. Studies of Semicircle Waveguide with Slot Radiator

Figures 14 and 15 show mathematical simulation results for microwave field emission conditions in the output of semicircle waveguide with slot radiator.

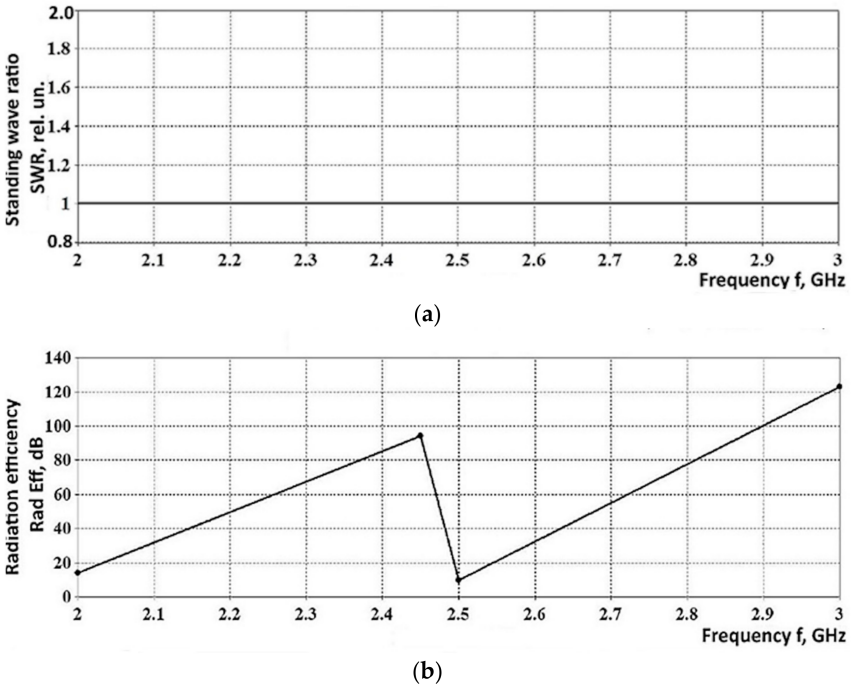

Figure 14. Efficiency indicators for semicircle waveguide: (**a**) standing wave ratio and (**b**) radiation efficiency.

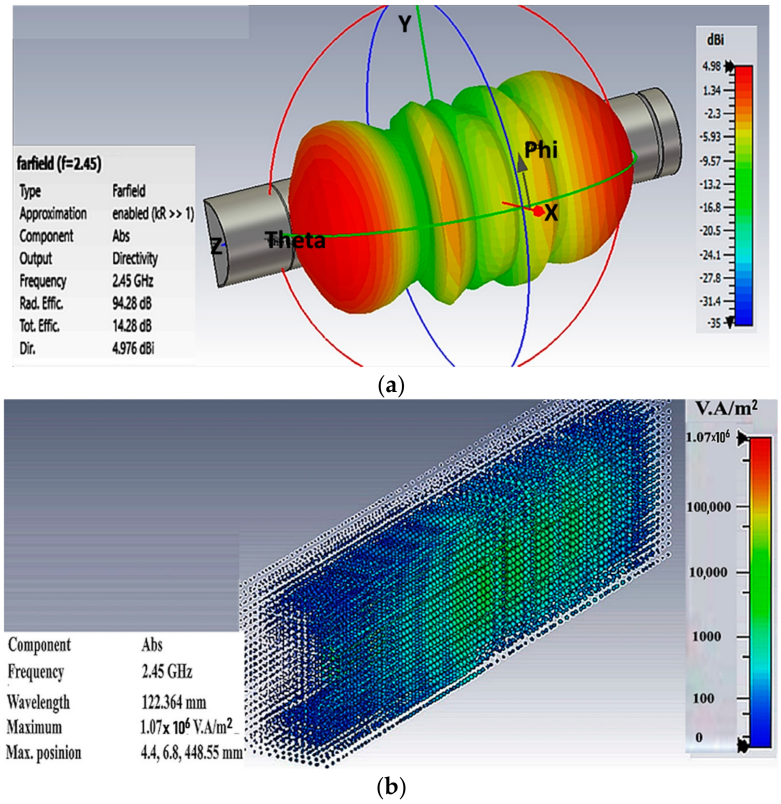

Figure 15. Results of 3D mathematical simulations for microwave field radiation in the output of semicircle waveguide with slot radiator: (**a**) 3D angular pattern for microwave electromagnetic field and (**b**) 3D density distribution of radiated microwave field.

3.4. Comparison of Radiation Patterns for the Three Types of Emitters Studied

A comparison of the radiation efficiency values for the three types of waveguides under study showed that the semicircular waveguide has the best data. However, the distribution of radiated power shown in Figures 11b, 13b and 15b does not fully allow us to estimate the change in the distribution of the electromagnetic field along the waveguides. Therefore, Figure 16 shows graphs of directional patterns for three types of waveguides.

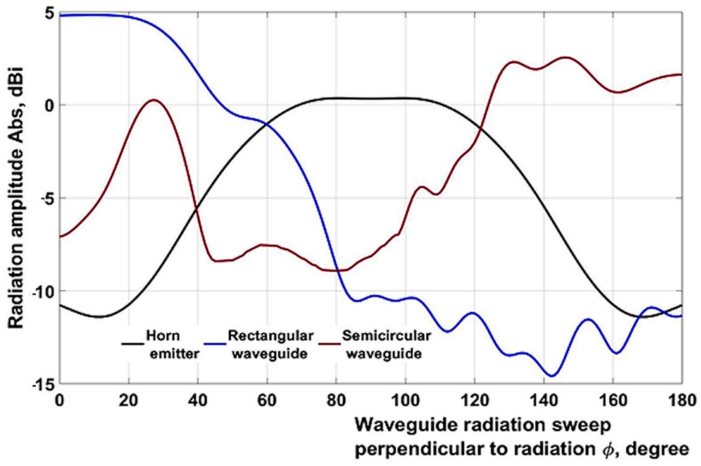

Figure 16. Radiation patterns for the three types of waveguides under study.

Figure 16 shows the radiation patterns along the waveguide perpendicular to the radiation. The radiation patterns show that the most uniform distribution of the microwave field is observed in a semicircular waveguide. This allows you to make a choice in its favor.

In order to confirm the authors' conclusion regarding the comparison of radiation uniformity based on the radiation pattern, further simulations were conducted. The distribution of the microwave field in the wheat grain layer with a moisture content of 14% was modeled. As a result, graphs (Figure 17) of the microwave field absorption along the length (*z*-coordinate) and height (*y*-coordinate) of the waveguide were obtained.

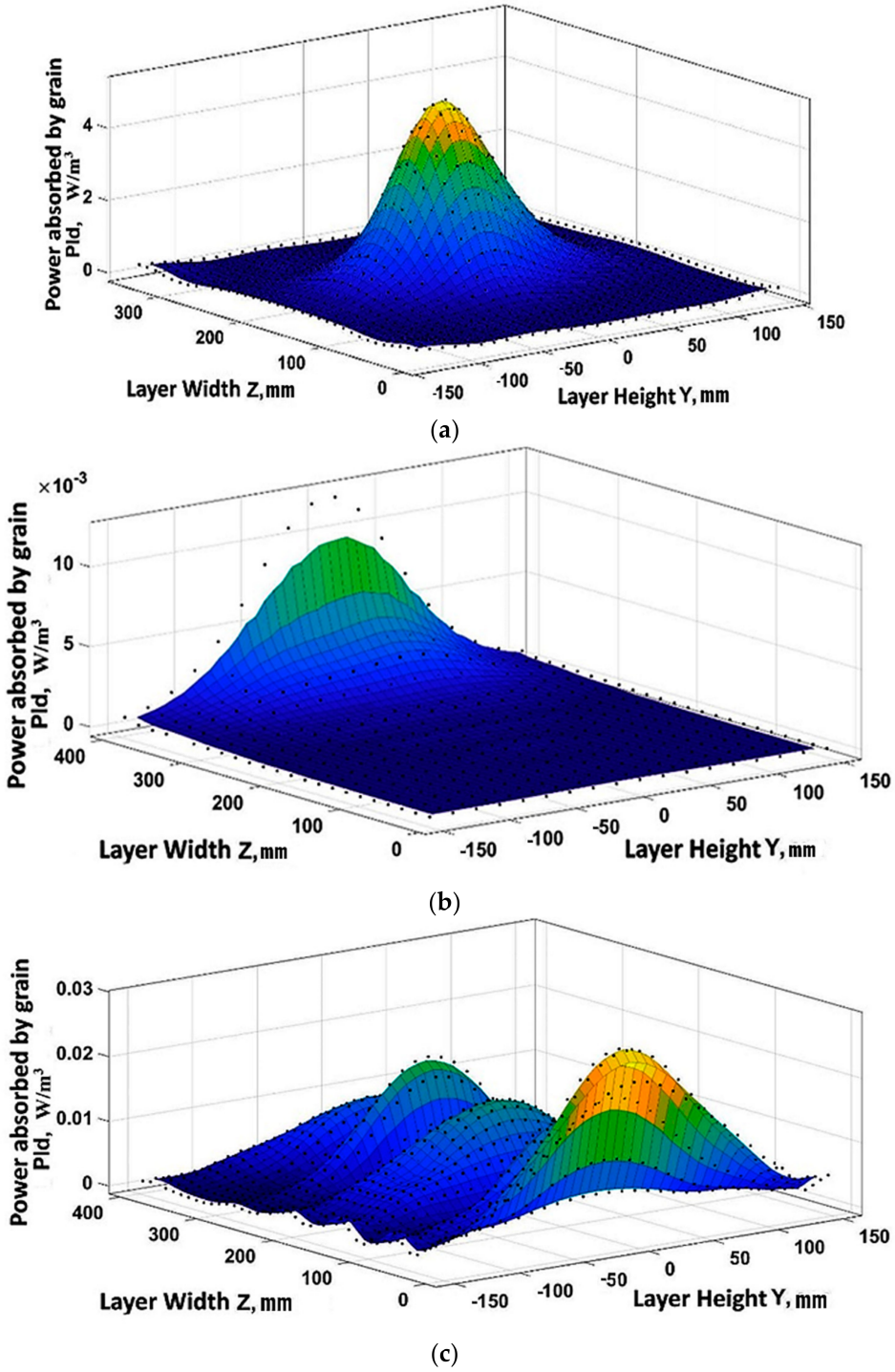

Figure 17. Grain absorption of the microwave field radiated by the waveguide (**a**) for a horn waveguide; (**b**) for a rectangular waveguide; and (**c**) for a semicircular waveguide.

The change in the power absorbed by the grain completely corresponds to the change in the radiation amplitude in the radiation patterns.

There is a significant difference in the irregularity of radiation between the three types of emitters. Therefore, it is not necessary to use numerical uniformity indices in this case. The use of homogeneity indices will be more meaningful when the difference between the radiation patterns of the electromagnetic field radiation is smaller.

It should be noted that in the microwave drying of grain, the operating modes of the radiators depend on the grain heating temperature and its current moisture content. The operating modes of the radiators are not constant but vary depending on the results of real-time monitoring of the grain layer's condition. Therefore, the coordination of waveguides is carried out based on the zone of operation within the setup (depending on the moisture content of the processed grain). The coordination of waveguides is assessed using three indicators: standing wave ratio, radiation efficiency, and uniformity of the microwave field distribution. The evaluation of coordination and "adjustment" of coordination is performed at the stage of modeling the field propagation in the grain. Thus, this work should be carried out in the next stage of modeling.

In this case, it will be necessary to consider the placement of waveguides in the microwave-active zone. The mutual arrangement of waveguides and the microwave-convective zone's enclosure will influence the modeling results. Once the best result is achieved through modeling, experimental studies can be conducted.

4. Discussion

Results of simulations show that a proper matching between the semicircular waveguide with the slot radiators makes it possible to attain values of SWR = 1, over the entire frequency range from 2 GHz to 3 GHz. The radiation efficiency of the electromagnetic field was 94.28 dB (see Figure 14b) compared to 94.43 dB, for the 55 × 110 rectangular waveguide. With the assumption that the radiation efficiency of semicircular waveguide was due to the absence of type E_{11} waves, we can conclude that their share is just 0.15 dB, which does not exceed 0.16% of the aggregate power transmitted through the waveguide.

It follows from the simulation results that the radiation efficiency for rectangular waveguides has a more uniform character in a wide range of waves. The radiation efficiency reduction in the range from 2 GHz to 3 GHz does not exceed 10%. In semicircular waveguides, the radiation efficiency changes stepwise, in this frequency range, and has its maximum value at its standard frequency of 2.45 GHz. Therefore, the operation conditions of magnetrons have to be tightly controlled, avoiding operation modes leading to their overheating, when semicircular waveguides are applied.

The overall efficiency of microwave energy transmission is 14.28 dB, for the semicircular waveguide (see Figure 15a), while that of the rectangular waveguide is 14.43 dB (see Figure 13a). At the same time, their radiation directionality features better uniformity compared to the 55 × 110 rectangular waveguides (see Figure 16).

In consideration of the issues discussed above, we may conclude that the application of more easily manufactured semicircular waveguides does not affect indicators of transmission efficiency and those of electromagnetic field distribution uniformity.

5. Conclusions

The characteristics obtained as a result of modeling (standing wave ratio, radiation efficiency and radiated power) for the types of microwave field emitters allowed for their evaluation and formulation of the following conclusions:

Application of horn-type waveguides in convective-microwave processing plants makes it possible to manufacture rather convenient processing equipment for processing grain. In the operating frequency range, their SWR is 1.3, and their radiation efficiency is 78 dB. However, such waveguides do not provide sufficient uniformity of microwave field distribution at their output affecting the efficiency of grain processing.

The use of rectangular 55 × 110 waveguides with a slot radiator makes it possible to ensure a more uniform radiation of electromagnetic field in the entire spectrum of wave types. Their SWR is equal to one, and the radiation efficiency amounts to 94.43 dB. At the

same time, their application requires further design development related to the issues of supplying the heat-carrier to the processing area.

Semicircular waveguides with a slot radiator feature SWR equal to one over the frequency range from 2 GHz to 3 GHz. Their radiation efficiency is 94.28 dB. The electromagnetic field distribution homogeneity of such waveguides is better compared to rectangular waveguides. Additionally, the problem of supplying the heat-carrier to the area of grain processing can be solved more easily for circular waveguides.

Based on the above, the authors have given preference to semicircular waveguides. Further research will be conducted with these types of emitters.

Author Contributions: Conceptualization, A.N.V.; methodology, D.B.; software, validation, formal analysis, A.A.V., A.N.V. and D.B.; investigation, A.A.V.; resources, data curation, A.N.V.; writing—original draft preparation, writing—review and editing, visualization, A.A.V.; supervision, project administration, A.N.V.; and funding acquisition, A.A.V. All authors have read and agreed to the published version of the manuscript.

Funding: This research was supported by Federal Scientific Agroengineering Center VIM (RF state assignment No FGUN-2022-0004).

Institutional Review Board Statement: Not applicable.

Informed Consent Statement: Informed consent was obtained from all subjects involved in the study.

Data Availability Statement: The research results are presented in the report on research work of the direction "Energy supply of agroindustrial complex" of FGBNU FNAC VIM for the 1st quarter of 2023.

Conflicts of Interest: The authors declare no conflict of interest.

References

1. Lermen, F.H.; Ribeiro, J.L.D.; Echeveste, M.E.; Martins, V.L.M.; Tinoco, M.A.C. Sustainable offers for drying and storage of grains: Identifying perceived value for Brazilian farmers. *J. Stored Prod. Res.* **2020**, *87*, 101579.
2. Coradi, P.C.; Lemes, Â.F.C.; Müller, A.; Jaques, L.B.A.; Dubal, Í.T.P.; Bilhalva, N.D.S.; Teodoro, P.E.; Steinhaus, J.I.; Maier, D.E. Silo-dryer-aerator in fixed and thick layer conceptualized for high quality of grains applied in different social scales post-harvest: Modeling and validation. *Dry. Technol.* **2020**, *40*, 1369–1394.
3. Binelo, M.O.; Faoro, V.; Kathatourian, O.A.; Ziganshin, B. Airflow simulation and inlet pressure profile optimization of a grain storage bin aeration system. *Comput. Electron. Agric.* **2019**, *164*, 104923. [CrossRef]
4. Khatchatourian, O.A.; Binelo, M.O.; Faoro, V.; Toniazzo, N.A. Three-dimensional simulation and performance evaluation of air distribution in horizontal storage bins. *Biosyst. Eng.* **2016**, *142*, 42–52. [CrossRef]
5. Dominika, B.; Anita, K.-P. Grained material drying in silo dryer. *Przem. Chem.* **2019**, *98*, 1913–1916.
6. De Camargo, D.; De Souza, G.; Franquelin, L.; Marcello, N. Study of tray and pulsed fluidized bed drying of brewer's spent grain. *Chem. Ind. Chem. Eng. Q.* **2019**, *25*, 229–237.
7. Supitchar, M.; Tawit, C. Dimensionless variable groups for the free-fall grain dryer. *Int. J. Agric. Biol. Eng.* **2019**, *12*, 197–204.
8. Van Hung, N.; Martinez, R.; Van Tuan, T.; Gummert, M. Development and verification of a simulation model for paddy drying with different flatbed dryers. *Plant Prod. Sci.* **2018**, *22*, 119–130. [CrossRef]
9. Rudobashta, S.; Zueva, G.; Zuev, N. Mathematical Modeling and Numerical Simulation of Seeds Drying Under Oscillating Infrared Irradiation Conference: 13th Polish Drying Symposium (PDS) Location: Kolobrzeg, POLAND Date: SEP 05-06, 2013. *Dry. Technol.* **2014**, *32*, 1352–1359.
10. Granella, S.J.; Bechlin, T.R.; Christ, D.; Coelho, S.R.M. Kinetic and physicochemical properties of drying-ozonation process on wheat grain. *J. Food Process. Preserv.* **2019**, *43*, e14057. [CrossRef]
11. Yogendrasasidhar, D.; Setty, Y.P. Drying kinetics, exergy and energy analyses of Kodo millet grains and Fenugreek seeds using wall heated fluidized bed dryer. *Energy* **2018**, *151*, 799–811. [CrossRef]
12. Albini, G.; Freire, F.B.; Freire, J.T. Barley: Effect of airflow reversal on fixed bed drying. *Chem. Eng. Process.-Process Intensif.* **2018**, *134*, 97–104.
13. Liu, C.; Chen, S.; Jiang, Y.; Wang, R.; Wu, W.; Zhou, H. The Principle and Experimental Research of New Type of Recirculating Grain Dryer. In Proceedings of the 2016 International Conference on Robots & Intelligent System (ICRIS), Zhangjiajie, China, 27–28 August 2016; pp. 453–456. [CrossRef]
14. Hemis, M.; Gariépy, Y.; Choudhary, R.; Raghavan, V. New coupling model of microwave assisted hot-air drying of a capillary porous agricultural product: Application on soybeans and canola seeds. *Appl. Therm. Eng.* **2017**, *114*, 931–937. [CrossRef]

15. Türkoğlu, T.; Baykal, H.; Yüksel, H.; Çalışkan Koç, G.; Dirim, S. The intermittent drying of wheat by microwave and fluidized bed drying. In Proceedings of the 21st International Drying Symposium (IDS), Valencia, Spain, 11–14 September 2018; pp. 1543–1550.
16. Bruce, R.M.; Atungulu, G.G.; Sadaka, S.; Smith, D. Impact of specific energy input of a 915 MHz microwave dryer on quality, functional, and physicochemical properties of different rice cultivars. *Cereal Chem.* **2021**, *98*, 557–570. [CrossRef]
17. Abano, E.E. Kinetics and Quality of Microwave-Assisted Drying of Mango (*Mangifera indica*). *Int. J. Food Sci.* **2016**, *2016*, 2037029. [CrossRef]
18. Walde, S.; Balaswamy, K.; Velu, V.; Rao, D. Microwave drying and grinding characteristics of wheat (*Triticum aestivum*). *J. Food Eng.* **2002**, *55*, 271–276. [CrossRef]
19. Bespalko, V.V.; Buryak, J.I. Efect of the pre-seeding treatment of seeds with the use of microwave field in combination with growth-promoter and bio-based product on sowing quality and crop productivity of summer barley. *Grain Legumes Cereal Crop.* **2014**, *12*, 133–138.
20. Kovalev, A.; Spiridonov, O.; Lysenko, I.; Ezhova, O. Method and System of Pre-Sowing Microwave Treatment of Agricultural Crop Seeds. *Int. J. Eng. Res. Technol.* **2020**, *13*, 3964–3969. [CrossRef]
21. Horuz, E.; Bozkurt, H.; Karataş, H.; Maskan, M. Simultaneous application of microwave energy and hot air to whole drying process of apple slices: Drying kinetics, modeling, temperature profile and energy aspect. *Heat Mass Transf.* **2017**, *54*, 425–436. [CrossRef]
22. Aghilinategh, N.; Rafiee, S.; Gholikhani, A.; Hosseinpur, S.; Omid, M.; Mohtasebi, S.S.; Maleki, N. A comparative study of dried apple using hot air, intermittent and continuous microwave: Evaluation of kinetic parameters and physicochemical quality attributes. *Food Sci. Nutr.* **2015**, *3*, 519–526. [CrossRef]
23. Vasilyev, A.A.; Vasilyev, A.N.; Budnikov, D.; Bolshev, V.; Shilin, D.; Shestov, D. Dynamic Arches Destruction by a Bulk Material Flow Separator: A Case Study of the Separator Usage in Microwave Grain Processing Plants. *Agronomy* **2022**, *12*, 997. [CrossRef]
24. Budnikov, D.A.; Vasilyev, A.N.; Vasilyev, A.A. *Designing Operation Areas of Convective-Microwave Processing Plants for Grain Treatment with the Application of Dynamoelectric Mathematical Simulations*; IOP Publishing: Oryol, Russia, 2022; 348p. (In Russian)
25. Vasiliev, A.N.; Goryachkina, V.P.; Dmitry, B. Research Methodology for Microwave-Convective Processing of Grain. *Int. J. Energy Optim. Eng.* **2020**, *9*, 1–11.
26. Li, Z.Y.; Wang, R.F.; Kudra, T. Uniformity Issue in Microwave Drying. *Dry. Technol.* **2011**, *29*, 652–660. [CrossRef]
27. Kolesnikov, S.M.; Trefilov, D.N.; Dementjev, A.N. Designing and optimization of stripline radiator radiator with the application of CST MICROWAVE STUDIO software. *Radioindustry* **2015**, *4*, 98–106.
28. Fateev, A.V. *Application of CST MICROWAVE STUDIO SW for Calculating Microwave Antennas Microwave Devices*; CST MICROWAVE STUDIO: Tomsk, Russia, 2017; p. 115.
29. Pozar; David, M. *Microwave Engineering*; University of Massachusetts at Amherst: Amherst, MA, USA, 2012; p. 756.
30. Yanushkevich, V.F. *Antennas and Microwave Devices*; PGU: Novopolotsk, Russia, 2009; p. 360.
31. Voskresensky, D.I.; Gostyukhin, V.L.; Maksimov, V.M.; Ponomaryov, L.I. *Microwave Devices and Antennas*; Radiotechnika: Moscow, Russia, 2008; 384p.
32. Pimenov, V.Y.; Volmn, V.I.; Murashov, A.D. *Technical Electrodynamics. M.: Radio and Communications*; Radio and Communications: Moscow, Russia, 2002; 536p.
33. Erokhin, G.A.; Chernyshov, O.V.; Kozyrev, N.D.; Kocherzhevsky, V.G. *Antenna-Feeder Devices ad Propagation of Radio Waves*; Erokhin, G.A., Ed.; Hot Line—Telecom: Moscow, Russia, 2004; 492p.
34. Smolders, A.B.; Visser, H.J.; Johannsen, U. *Modern Antennas and Microwave Circuits—A Complete Master-Level Course*; Eindhoven University of Technology: Eindhoven, The Netherlands, 2019; p. 165.
35. Nechaev, Y.B.; Nikolaev, V.I.; Andreev, R.N.; Vinokurova, N.N. *Antennas, Microwave Devices and Their Technologies*; OAO Concern 'Sozvezdie': Voronezh, Russia, 2008; 629p.
36. Rfrliner, M.M. *Electrodynamics of Microwave*; Novosibirsk State University : Novosibirsk, Russia, 2006; 258p.
37. Inan, U.S.; Marshall, R.A. *Numerical Electromagnetics*; The FDTD Method; Cambridge University Press: New York, NY, USA, 2011; 406p.
38. Chapman, S.J. *MATLAB Programming for Engineers*; Thomson Learning: Toronto, ON, Canada, 2015; 592p.
39. Petrov, R.V. Studies of magneto-electric slot-type resonator for microwave frequency range. *Eng. Phys.* **2012**, *1*, 33–38. (In Russian)
40. Zavaliy, A.A.; Volozhaninov, S.S.; Volozhaninov, N.V. Designing slot-type microwave radiator for treatment soil, seeds and plants. In *Collected Book: Innovative Technologies in Science and Education (Conf. 'ITNO 2022')*; Collection of Research Papers of the X Jubilee Int. Research-to-Practice Conference; Limited Liability Company "DGTU-PRINT": Rostov-on-Don, Russia, 2022; pp. 69–74.
41. Topolski, J.A. *Computational Analyses of High Power Microwave Slotted Array Antennas for Mobile Applications*; B.S. Electrical Engineering; The University of New Mexico: Albuquerque, NM, USA, 2007; p. 179.

Disclaimer/Publisher's Note: The statements, opinions and data contained in all publications are solely those of the individual author(s) and contributor(s) and not of MDPI and/or the editor(s). MDPI and/or the editor(s) disclaim responsibility for any injury to people or property resulting from any ideas, methods, instructions or products referred to in the content.